Planar Double-sided Printed quasi-Yagi Antenna with Enhanced Impedance Bandwidth and Reduced Size for Wideband Wireless Applications

Tian Li[1, *], Fu-Shun Zhang[1], Fei Gao[2], and Yan-Li Guo[3]

Abstract—A compact wideband planar double-sided printed quasi-Yagi antenna is presented. This paper focuses on the feasibility of substituting conventional balun for microstrip-to-slotline transition balun to achieve wider bandwidth and relatively smaller size. The proposed antenna, consisting of a feeding balun, a concave arc-shaped reflector, a modified driver with stacked structure and two directors, is designed and fabricated. Good agreement between simulated and measured results is observed. Simulation and measurement results reveal that the proposed antenna can provide an impedance bandwidth of nearly 100% (2.02–6.05 GHz). Additionally, within the impedance bandwidth, the radiation pattern of the proposed antenna has front-to-back (F/B) ratios ranging from 10.1 dB to 19.1 dB, cross-polarization levels in the main radiation direction from 19.8 dB to 36.2 dB and gains from 3.4 dBi to 7.4 dBi.

1. INTRODUCTION

Planar quasi-Yagi antennas have attracted great attention due to their merits of simple structure, low profile, light weight, low fabrication cost, broad bandwidth, realizing unidirectional radiation with high gain, and suitability for integration with microwave circuits. Since the driver element of a planar quasi-Yagi antenna is a balanced structure, whereas the feeder is usually an unbalanced coaxial cable, to broaden the impedance bandwidth of the antenna, various techniques in [1–9] focus on the balanced-to-unbalanced (balun) transition structures, including coplanar waveguide (CPW)-to-slotline transition balun [1, 2], microstrip-to-coplanar stripline (CPS) transition balun [3–5], microstrip-to-slotline transition balun [6–8] and a novel integrated balun with stepped impedance coupled structure [9]. Many newly published references, such as [6–8], are inclined to employ microstrip-to-slotline transition balun structures to obtain stable radiation pattern and gain within a large bandwidth. However, relatively few designs of the planar quasi-Yagi antennas on the basis of the conventional balun have been reported. Actually, when substituting conventional balun for microstrip-to-slotline transition balun and properly modifying the driver, reflector and parasitic directors simultaneously, a better performance in bandwidth and size can be obtained.

Substituting conventional balun for microstrip-to-slotline transition balun will allow the planar quasi-Yagi antenna to be double-sided printed in overall structure, which facilitates its obtaining relatively larger bandwidth and more stable radiation pattern. For demonstration, a planar double-sided printed quasi-Yagi antenna is presented in this paper. It is based on a conventional balun and designed to enhance both the bandwidth and gain. In order to enhance its bandwidth, a double-sided printed driver dipole is introduced. Meanwhile, the driver's stacked structure will miniaturize its dependence on the antenna lateral dimension. A concave arc-shaped reflector is employed to diminish

the antenna lateral dimension, which can also compensate the gain decrease caused by the reduced antenna lateral dimension, especially for the lower band. To further enhance the gain, the second-stage director consists of two parasitic elements. The spacing between two elements is chosen to be larger to obtain a wide aperture length, thus achieving an increased gain. In addition, the measured results have a reasonable agreement with the simulated ones.

2. ANTENNA CONFIGURATION

As shown in Figure 1, the proposed antenna can be divided into four parts, namely feeding balun, driver, reflector and two directors. The substrate for the proposed antenna is $63\,\text{mm} \times 60\,\text{mm} \times 1.8\,\text{mm}$ in size, and its relative dielectric constant and the loss tangent are 2.2 and 0.0009, respectively. The feeding balun is a conventional exponentially tapered balun and 39 mm in length. The driver consists of two pairs of rectangular arms. They are printed on the front and back sides of the substrate respectively and connected with two shorting vias [10]. Meanwhile, the overall size of the front and back arms are $29\,\text{mm} \times 3\,\text{mm}$ and $22\,\text{mm} \times 13.7\,\text{mm}$, respectively. The concave arc-shaped reflector is printed on the back side of the substrate and truncated with a proper distance from the feeding port. The radius of its arc-shaped aperture is 58.8 mm. The director consists of two stages. The first-stage director has only one parasitic element, while the second-stage director consists of two parasitic elements. A coupling microstrip line is introduced between two parasitic elements of the second-stage director to enhance their coupling. Furthermore, all the parasitic director elements as well as the coupling microstrip line are symmetrically printed on both the front and back sides of the substrate. All the parasitic director elements are connected with shorting vias and have a same size of $14\,\text{mm} \times 3\,\text{mm}$. The coupling microstrip line is $6\,\text{mm} \times 3\,\text{mm}$ in size. In addition, two rectangular slots are symmetrically etched on the front feeding microstrip line to reach a good impedance matching [11]. The detailed geometry and dimensions of the proposed antenna are given in Figure 1 and Table 1.
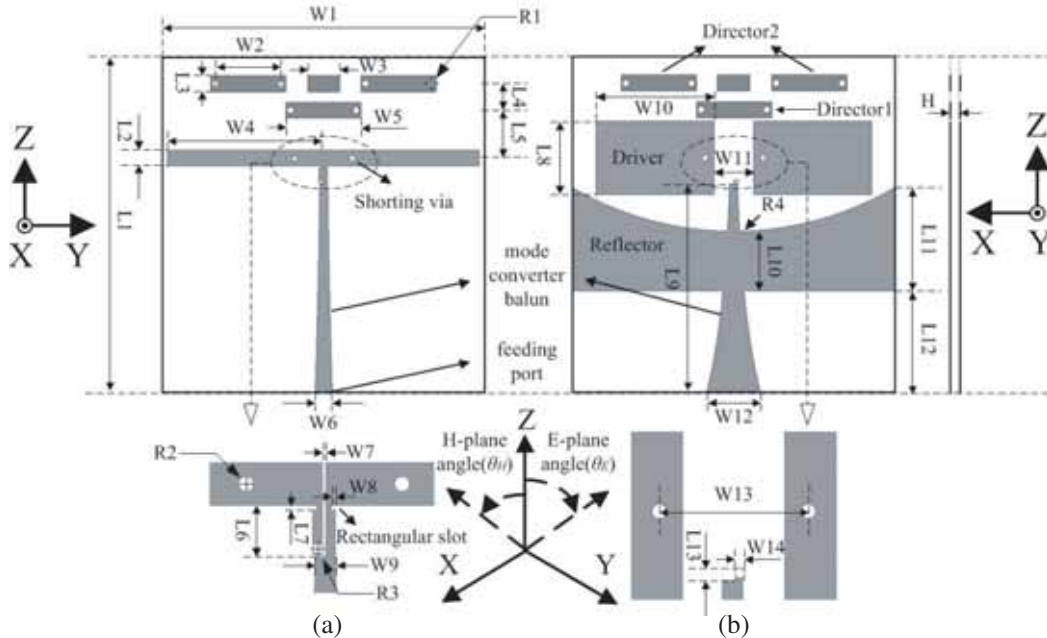
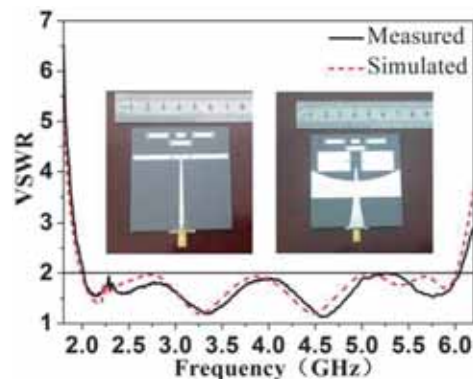**Figure 1.** Configuration of the proposed antenna. (a) Front view; (b) Back view;(c) Side view.

3. ANTENNA DESIGN

A conventional exponentially tapered balun is used for unbalance-balance transition, namely transition from the coaxial cable to the driver of the proposed planar quasi-Yagi antenna [12]. Meanwhile, it

Table 1. Dimensions of the proposed antenna.

Parameter	Value (mm)	Parameter	Value (mm)	Parameter	Value (mm)
$L1$	63	$L12$	19	$W10$	22
$L2$	3	$L13$	0.9	$W11$	7.36
$L3$	3	$W1$	60	$W12$	10
$L4$	5	$W2$	12.24	$W13$	10.76
$L5$	9	$W3$	6	$W14$	0.7
$L6$	3.5	$W4$	29	R1	0.6
$L7$	0.3	$W5$	14	R2	0.5
$L8$	13.7	$W6$	3.2	R3	0.35
$L9$	39	$W7$	0.2	R4	58.8
$L10$	11.2	$W8$	0.3	H	1.8
$L11$	19.45	$W9$	1.44		

can convert coaxial cable transmission mode (TEM) to the balanced microstrip transmission mode (quasi-TEM) gradually; thus it can achieve impedance matching. The driver is energized directly by the balun while the reflector and directors act as parasitic radiators whose current are induced by mutual coupling. Thus, the bandwidth of the driver greatly determines the bandwidth of the proposed planar quasi-Yagi antenna. With the stacked structure, the impedance and pattern bandwidths of the driver dipole can be improved significantly. The front and back arms are designed for the lower and upper bands, respectively. When the lower resonant frequencies are properly close to the upper resonant frequencies, the impedance bandwidth will be significantly broadened. Moreover, the reflector is used to reflect the transverse-electric surface wave generated by the driver. In this design, a concave arc-shaped reflector is employed instead of a conventional straight reflector. This structure not only facilitates the concentration of the radiation towards the end-fire direction, but also equivalently increases the length of the reflector aperture, which enables the end-fire radiation patterns at lower band to stay stable without significant degradation. Furthermore, the parasitic directors are used to achieve a very substantial increase with respect to gain in the forward end-fire direction compared with a simple driver. To obtain a larger aperture size, the spacing between two second-stage parasitic elements is chosen to be larger. In addition, in order to compensate the coupling between the two elements caused by their larger spacing, a coupling microstrip line is introduced. Finally, two rectangular slots symmetrically loaded on the front feeding microstrip line act as a perturbation structure to adjust the impedance matching.

Figure 2. Simulated and measured VSWRs and the photographs of the fabricated antenna.

4. SIMULATED AND MEASURED RESULTS

In order to facilitate the manufacture, the proposed antenna with the parameters shown in Figure 1 is fabricated and measured. The measured and simulated VSWRs of the proposed antenna are depicted in Figure 2. Good agreement between the simulated and measured results is obtained. With reference to the figure, the simulated and measured impedance bandwidths (VSWR $\leq$ 2) of the proposed antenna are 100.5% (1.99–6.01 GHz) and 99.9% (2.02–6.05 GHz), respectively. In addition, the measured bandwidth of nearly 100% (2.02–6.05 GHz) not only meets the need for certain Wi-Fi (2.4/5.2/5.8 GHz) or WiMAX (2.5/3.5/5.5 GHz) band communication application, but also provides the potential to implement multiservice transmission. Moreover, simulated radiation properties of the proposed antenna are shown in Table 2 and Figure 3. It is seen that relatively stable pattern characteristics are obtained within the operating band.

**Table 2.** Simulated radiation properties of the proposed antenna.

Freq. (GHz)	3 dB beam width (°)		X pol. level in the main radiation direction (dB)	F/B ratio (dB)	Deviation angle in E-plane (°)	Gain (dB)
	E-plane	H-plane				
2	87	204	29.3	10.3	+9	3.6
2.5	86	168	36.6	14.0	+6	3.8
3	87	196	28.8	10.1	+5	4.1
3.5	88.5	189.5	25.9	10.8	+5	4.4
4	71.5	168	26.4	14.6	+3	5.1
4.5	60	134.5	25.5	19.1	+2.5	6.7
5	55	107	23.3	14.5	0	6.9
5.5	46	87.5	21.8	11.2	−1.5	7.7
6	33	101	19.8	15.7	1	7.9

Figure 3 shows the simulated and measured radiation patterns in the E-plane (YZ-plane) and H-plane (XZ-plane) at 2.5, 4.0 and 5.5 GHz. Compared with the simulated radiation properties shown in Table 2, the measured radiation patterns at 2.5, 4.0 and 5.5 GHz have the E-plane 3-dB beamwidths of 84.6°, 71.2° and 65°, H-plane 3-dB beamwidths of 148.4°, 134° and 75.2°, cross-polarization levels in the main radiation direction of 36.2 dB, 27.3 dB and 20.9 dB, front-to-back (F/B) ratios of 14.5 dB, 17.3 dB and 10.3 dB and deviation angles in the E-plane of +5°, 2° and −3°, respectively. In Figure 4, the measured gains and F/B ratios are from 3.4 dBi to 7.4 dBi with an average gain of 5.3 dBi and 10.5 dB to 17.3 dB with an average F/B ratio of 13.0 dB, respectively. Additionally, it should be noted that the discrepancy between the simulated and measured results may be caused by the imperfect testing environment. Furthermore, the error in the process of fabrication and the presence of the SMA connector interfering with the radiated field may be taken into account as well.

A comparison of the proposed antenna with published reference work is made in terms of operating frequency band, relative dielectric constant of the substrate, antenna size, bandwidth and gain with results presented in Table 3. The selected criteria for inclusion in this comparison are newly published wideband planar quasi-Yagi antennas. From Table 3, it could be seen that the proposed antenna provides a wider operating bandwidth with a relatively reduced size. Furthermore, the substrate relative dielectric constant and loss tangent of the proposed antenna is lower compared with that of other reference antennas, which contributes to a better performance.

5. PARAMETRIC STUDY

All critical physical parameters, such as $W4$, $W10$, $L9$, $L7$, $L12$ and $L5$, should be adjusted carefully to achieve a good performance. In this section, the effects of these parameters on impedance bandwidth and F/B ratio are examined. During this process, all the other parameters not mentioned stay constant as shown in Table 1.
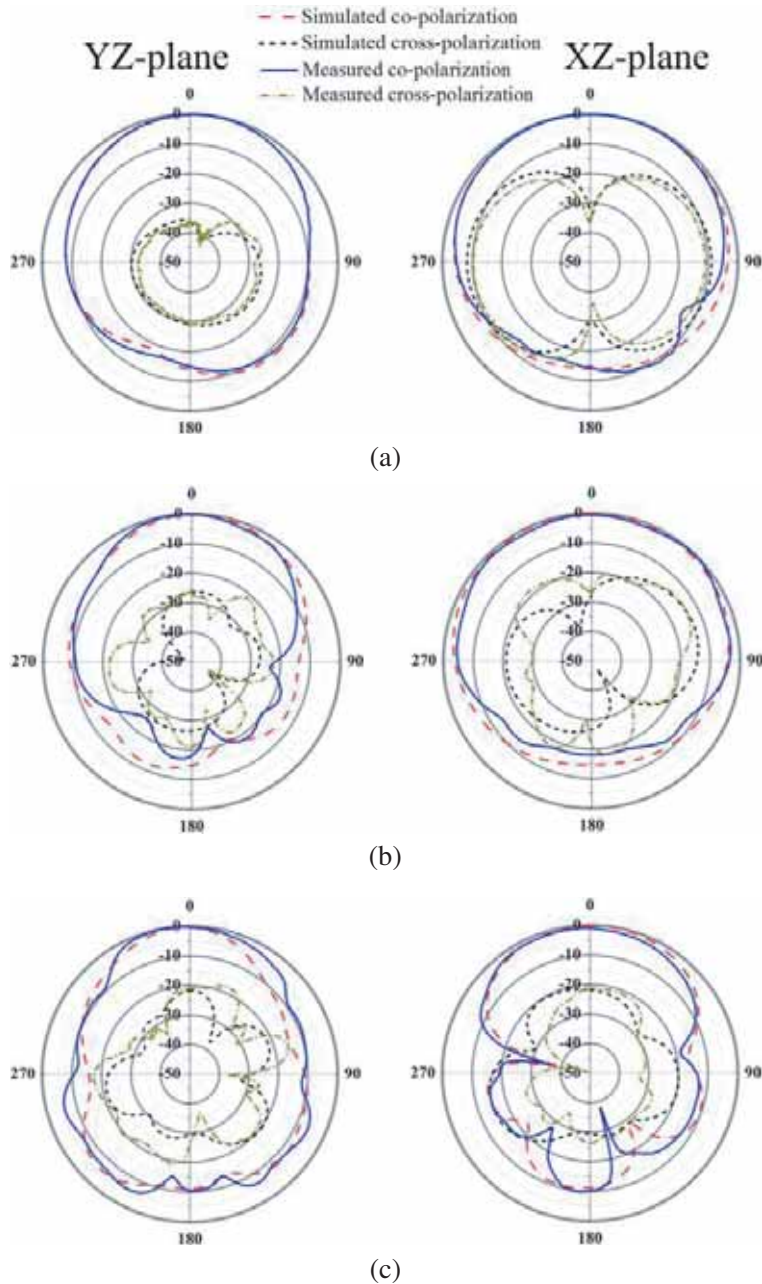
Figure 3. Simulated and measured radiation patterns in the E-plane (YZ-plane) and H-plane (XZ-plane). (a) 2.5 GHz; (b) 4 GHz ; (c) 5.5 GHz.

5.1. Effect of the Front and Back Arms of the Driven Dipole ($W4$ and $W10$)

The effects of the lengths of the front and back arms ($W4$ and $W10$) on the impedance bandwidth are shown in Figure 5 and Figure 6, respectively. As expected, as $W4/W10$ increases/decreases, the lower/upper resonant frequencies shift toward lower/upper band, while the upper/lower resonant frequencies almost stay the same. The results indicate that the impedance bandwidth at lower/upper frequencies is mainly related to the lengths of the front and back arms. To obtain good matching, $W4$ and $W10$ are set as 29 mm and 22 mm, respectively.
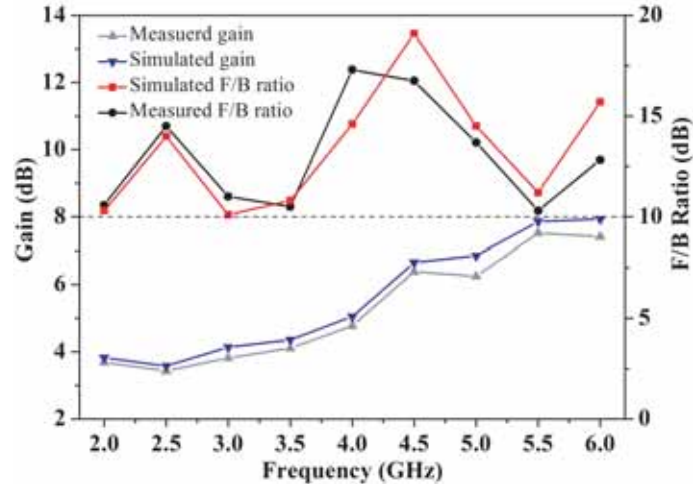
Figure 4. Simulated and measured gains and F/B ratios of the proposed antenna.

Table 3. Performance comparisons between the proposed and referenced antennas.

| Reference Designs	Operating Freq. (GHz)	Substrate ε	Antenna size length $\times$ width $\times$ leight (mm^3)	bandwidth	Gain (dBi)
Proposed Antenna	2.02–6.05	2.2	$63 \times 60 \times 1.8$ ($0.84\lambda_0 \times 0.80\lambda_0 \times 0.02\lambda_0$)	3.0 : 1	3.4–7.4
Wu et al. [6]	3.8–10.3	4.4	$36 \times 35 \times 0.5$ ($0.85\lambda_0 \times 0.82\lambda_0 \times 0.01\lambda_0$)	2.7 : 1	4.1–7.0
Yeo and Lee [7]	1.62–2.96	4.4	$115 \times 90 \times 1.6$ ($0.88\lambda_0 \times 0.69\lambda_0 \times 0.01\lambda_0$)	1.8 : 1	4.5–5.5
Ta et al. [8]	4.64–7.42	10.2	$60 \times 50 \times 0.635$ ($1.21\lambda_0 \times 1.01\lambda_0 \times 0.01\lambda_0$)	1.6 : 1	6.0–6.75
Abbosh [9]	4.7–10.4	10.2	$27 \times 32 \times 0.64$ ($0.68\lambda_0 \times 0.81\lambda_0 \times 0.02\lambda_0$)	2.2 : 1	3.6–4.5
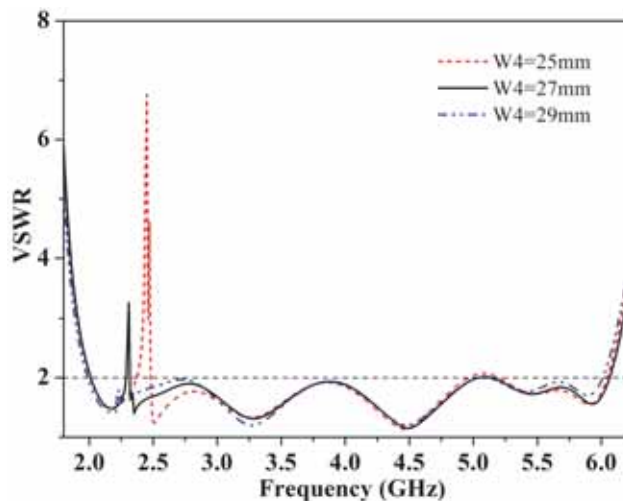
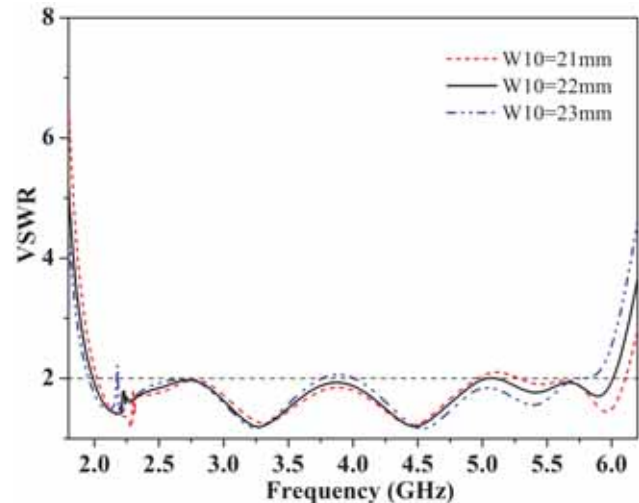**Figure 5.** Simulated VSWRs with varied $W4$.

Figure 6. Simulated VSWRs with varied $W10$
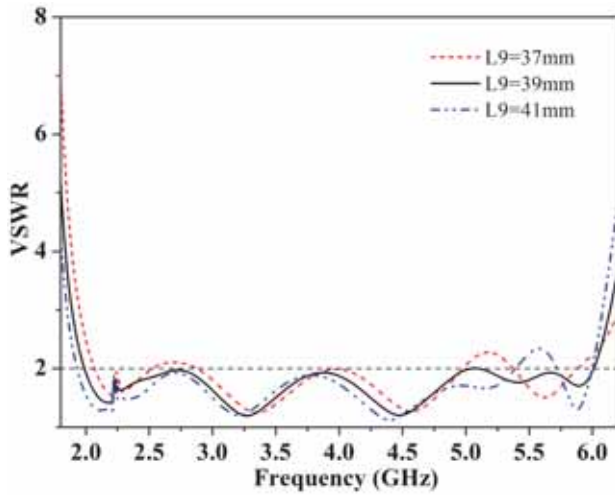
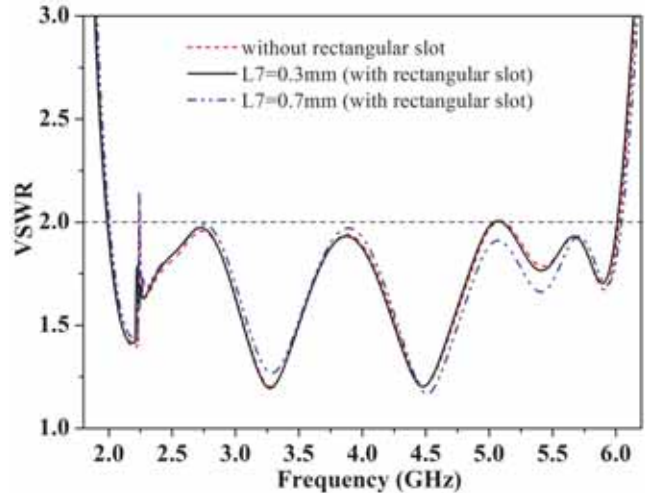**Figure 7.** Simulated VSWRs with varied $L9$.
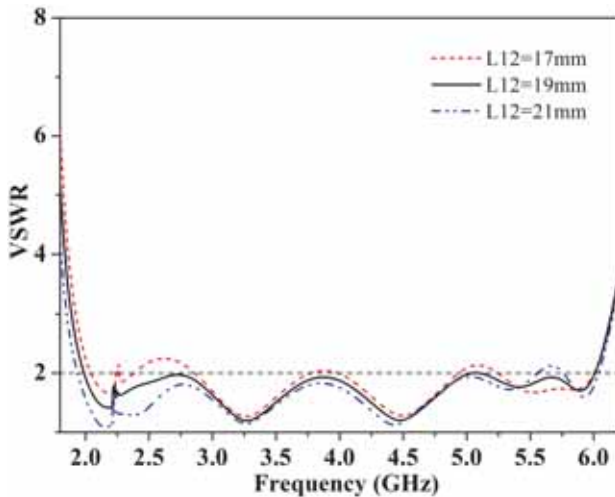

Figure 8. Simulated VSWRs with varied $L7$.
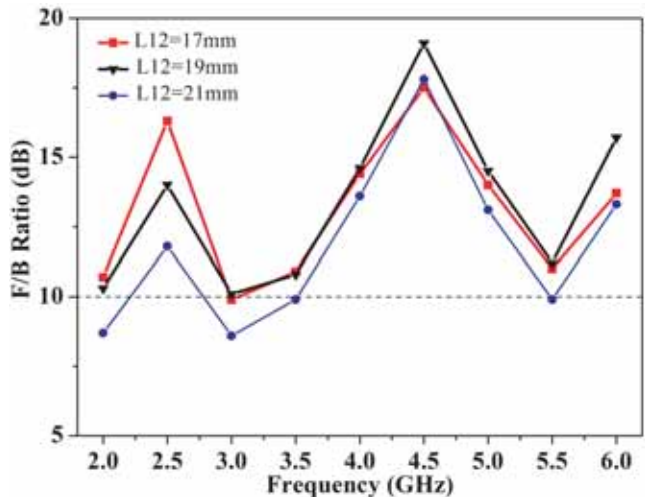

Figure 9. Simulated VSWRs with varied $L12$.

Figure 10. Simulated F/B ratios with varied $L12$.

5.2. Effect of the Mode Converter Balun and the Rectangular Slots ($L9$ and $L7$)

Figure 7 and Figure 8 reveal the influence of the lengths of the balun and rectangular slots ($L9$ and $L7$) on the impedance bandwidth, respectively. As $L9$ increases, though the impedance bandwidth at lower frequencies is broadened, the impedance matching at higher frequencies will be deteriorated, whether the value increases or decreases. To obtain good impedance matching, the balun length $L9$ is set to 39 mm. Moreover, as shown in Figure 8, without the rectangular slots loaded on the front feeding microstrip line, a singular point of VSWR at a lower frequency occurs. When the rectangular slots are introduced with discreetly optimized lengths of 0.3 mm, the VSWR singular point will be eliminated.

5.3. Effect of the Reflector and the Directors ($L12$ and $L5$)

$L12$ means the truncated length of the reflector from the feeding point. Both the impedance bandwidth and F/B ratio are sensitive to $L12$. As shown in Figure 9 and Figure 10, as $L12$ increases, its impedance bandwidth will be broadened, while the performance of F/B ratio will degrade significantly, especially for lower frequencies. $L5$ means the spacing between the first-stage director and the driver. As shown
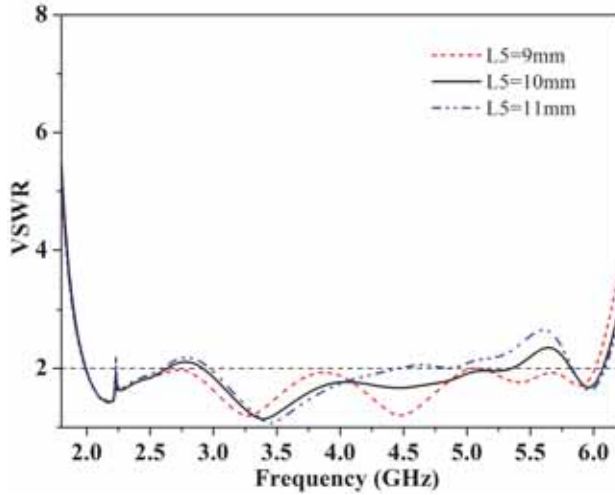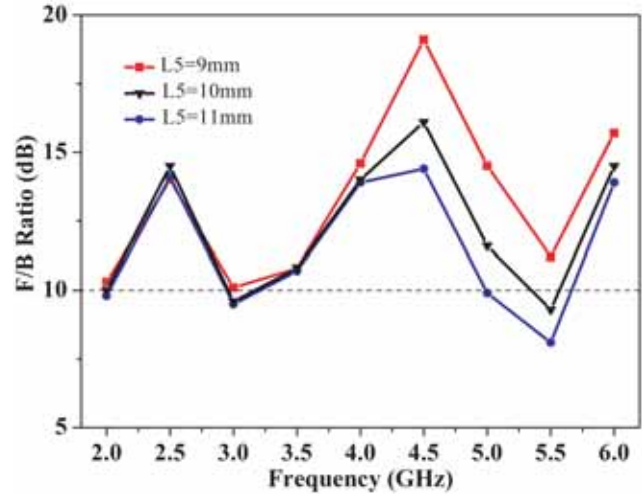
Figure 11. Simulated VSWRs with varied $L5$.   **Figure 12.** Simulated F/B ratios with varied $L5$.

in Figure 11 and Figure 12, as $L5$ increases, the performance of the impedance bandwidth and F/B ratio will be deteriorated, especially for higher frequencies. To obtain good matching and F/B ratio, $L12$ and $L5$ are set as 19 mm and 9 mm, respectively.

6. CONCLUSION

A planar double-sided printed quasi-Yagi antenna with enhanced impedance and reduced size has been presented. Simulation and measurement results indicate that fed by a conventional balun, the proposed antenna can produce an impedance bandwidth of nearly 100% (2.02–6.05 GHz). Meanwhile, within the operating bandwidth, good F/B ratios and cross-polarization levels in the main radiation direction, which are better than 10.1 dB and 19.8 dB, respectively, are obtained. Relatively moderate gains, ranging from 3.4 dBi to 7.4 dBi with an average gain of 5.3 dBi, are obtained simultaneously. With these inherent characteristics, the proposed antenna can be a good candidate for wideband wireless applications.

REFERENCES

1. Sor, J., Y. Qian, and T. Itoh, "Coplanar waveguide fed quasi-Yagi antenna," *Electron. Lett.*, Vol. 36, No. 1, 1–2, 2000.
2. Ding, Y., Y.-C. Jiao, P. Fei, B. Li, and Q. Zhang, "Design of a multiband quasi-Yagi-type antenna with CPW-to-CPS transition," *IEEE Antennas Wireless Propag. Lett.*, Vol. 10, 1120–1123, 2011.
3. Kaneda, N., W. R. Deal, Y. Qian, R. Waterhouse, and T. Itoh, "A broadband planar quasi-Yagi antenna," *IEEE Trans. Antennas Propag.*, Vol. 50, No. 8, 1158–1160, Aug. 2002.
4. Han, K., Y. Park, H. Choo, and I. Park, "Broadband CPS-fed Yagi-Uda antenna," *Electron. Lett.*, Vol. 45, No. 24, 1207–1209, Nov. 2009.
5. Nikolic, N. and A. Weily, "Compact E-band planar quasi-Yagi antenna with folded dipole driver," *IET Microw. Antennas Propag.*, Vol. 4, No. 11, 1728–1734, 2010.
6. Wu, J. N., Z.-Q. Zhao, Z.-P. Nie, and Q.-H. Liu, "Design of a wideband planar printed quasi-Yagi antenna using stepped connection structure," *IEEE Trans. Antennas Propag.*, Vol. 62, No. 6, 3431–3435, Jun. 2014.
7. Yeo, J. and J.-I. Lee, "Broadband compact series-fed dipole pair antenna with simplified integrated balun," *Microwave Opt. Technol. Lett.*, Vol. 56, No. 8, 1731–1734, Jul. 2014.
8. Ta, S. X., B. Kim, H. Choo, and I. Park, "Wideband quasi-Yagi antenna fed by microstrip-to-slotline transition," *Microwave Opt. Technol. Lett.*, Vol. 54, No. 1, 150–153, Jul. 2012.

9. Abbosh, A., "Ultra-wideband quasi-Yagi antenna using dual-resonant driver and integrated balun of stepped impedance coupled structure," *IEEE Trans. Antennas Propag.*, Vol. 61, No. 7, 3885–3888, Jul. 2013.

10. Liu, J.-H., S.-Y. Zheng, Y.-X. Li, and Y.-L. Long, "Broadband monopolar microstrip patch antenna with shorting vias and coupled ring," *IEEE Antennas Wireless Propag. Lett.*, Vol. 13, 39–42, 2014.

11. Deshmukh, A. A. and K. P. Ray, "Formulation of resonance frequencies for dual-band slotted rectangular microstrip antennas," *IEEE Mag. on Antenna Propag.*, Vol. 54, 78–97, 2012.

12. Mirzapour, M. I., S. M. J. Razavi, and S. H. Mohseni Armaki, "Ultra-wideband planar LPDA antenna with mode converter balun," *Electron. Lett.*, Vol. 50, No. 12, 848–850, Jun. 5, 2014.